

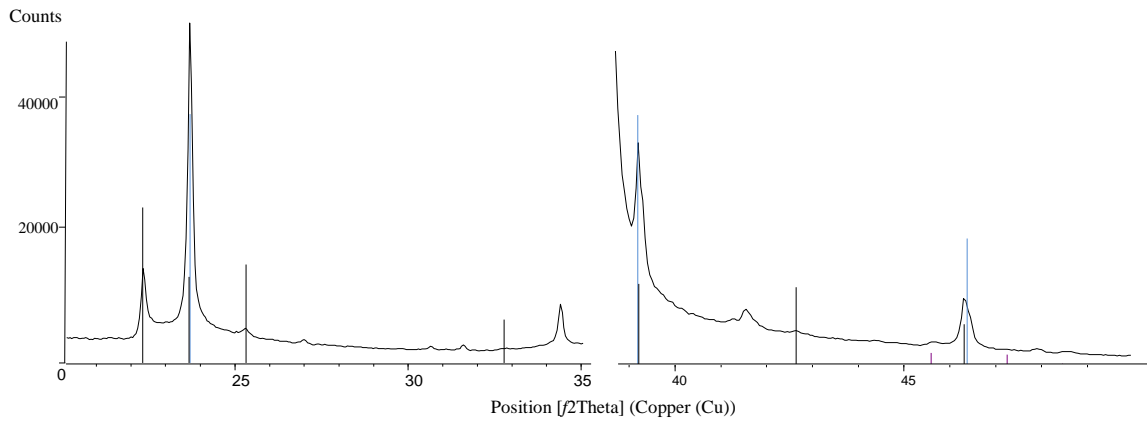
## SUPPORTING INFORMATION

### **A NEW INTEGRATED TLC/MU-ATR/SERS ADVANCED APPROACH FOR THE IDENTIFICATION OF TRACE AMOUNTS OF DYES IN MIXTURES.**

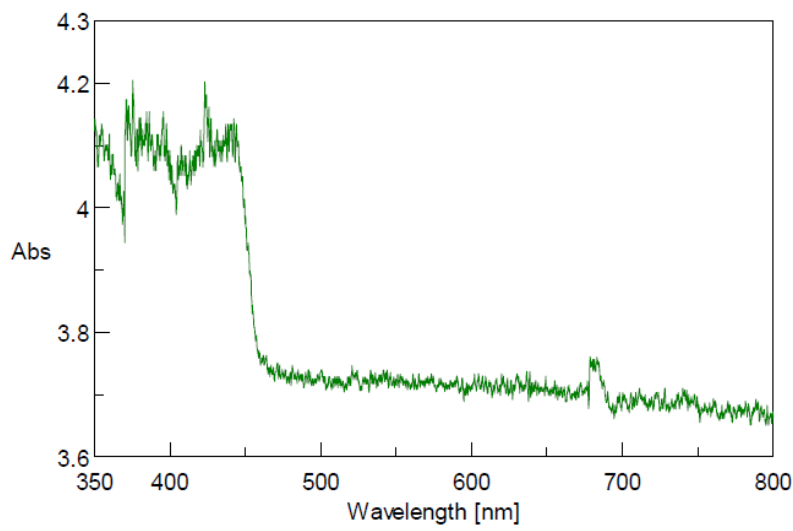
Giorgia Sciutto<sup>1</sup>, Silvia Prati<sup>1</sup>, Irene Bonacini<sup>1</sup>, Lucio Litti<sup>2</sup>, Moreno Meneghetti<sup>2</sup>, Rocco Mazzeo<sup>1</sup>

<sup>1</sup> Microchemistry and Microscopy Art Diagnostic Laboratory, Department of Chemistry, University of Bologna, Via Guaccimanni 42, 48121, Ravenna.

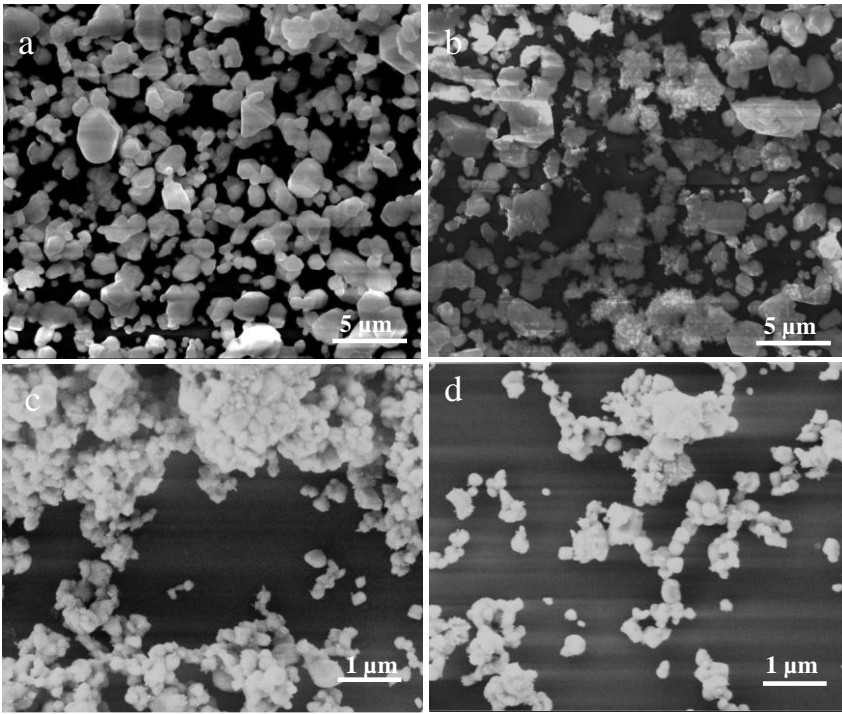
<sup>2</sup> Department of Chemical Science, University of Padova, via Marzolo 1, 35131, Padova.



**SI Figure 1.** XRD diffractogram of AgI particles deposited on an Au substrate.

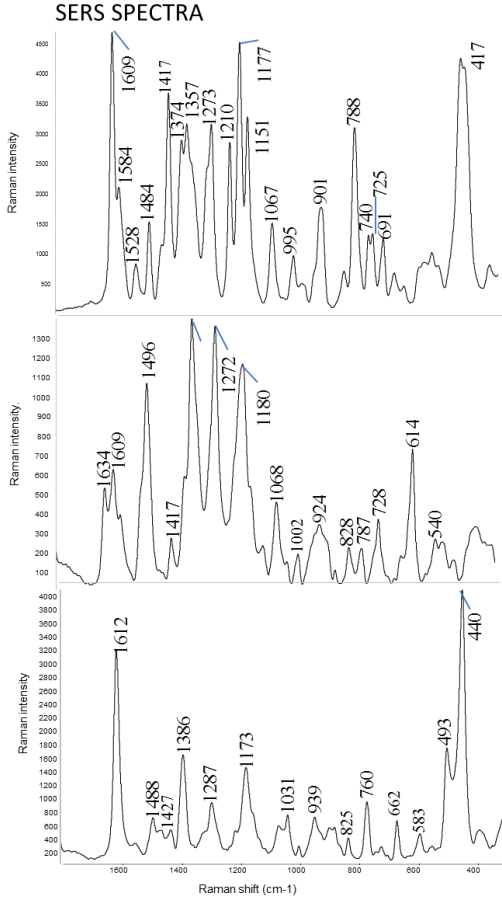


**SI Figure 2.** UV-Vis spectra of AgI suspension in 2-propanol ([AgI]: 0.014 g/mL)

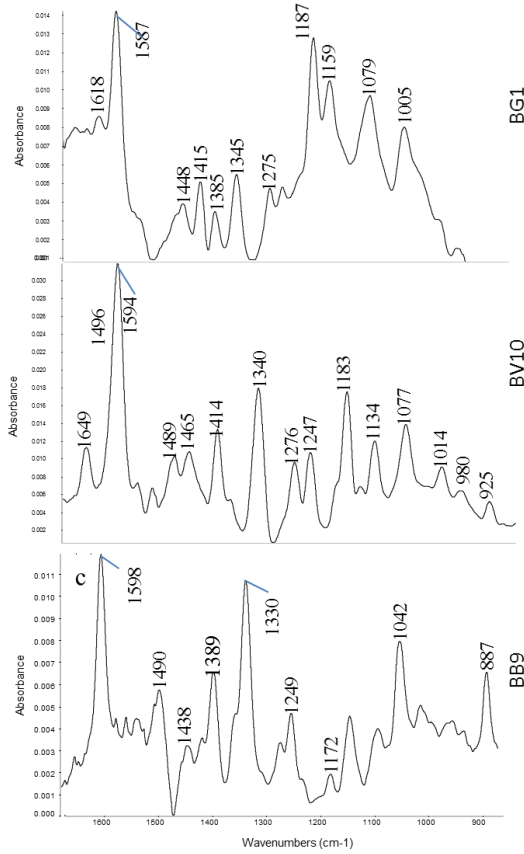


**SI Figure 3.** SEM images of AgI@SiO<sub>2</sub> substrate before (a, c) and after (b, d) laser irradiation

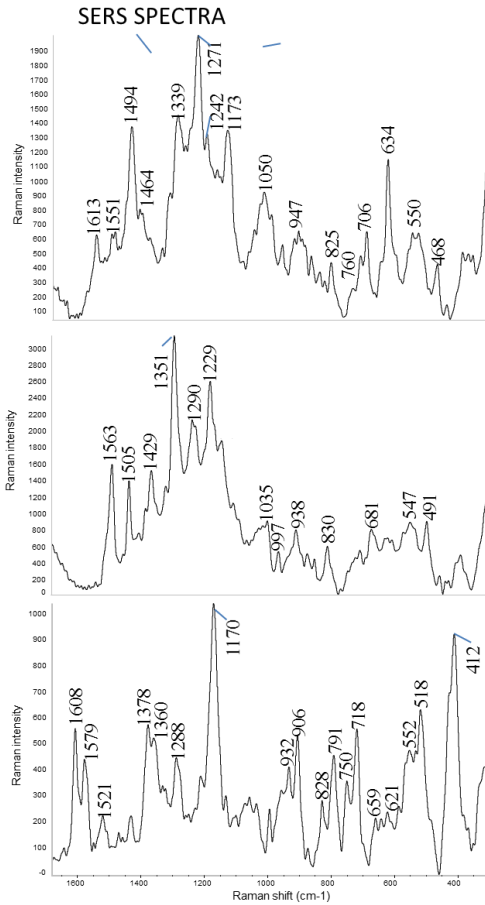
# DYE MIXTURE A



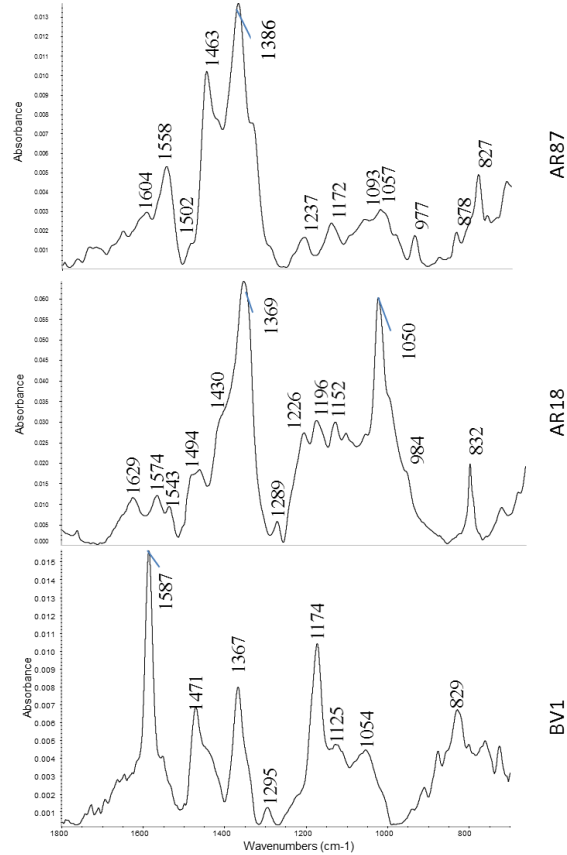
### MU-ATR SPECTRA



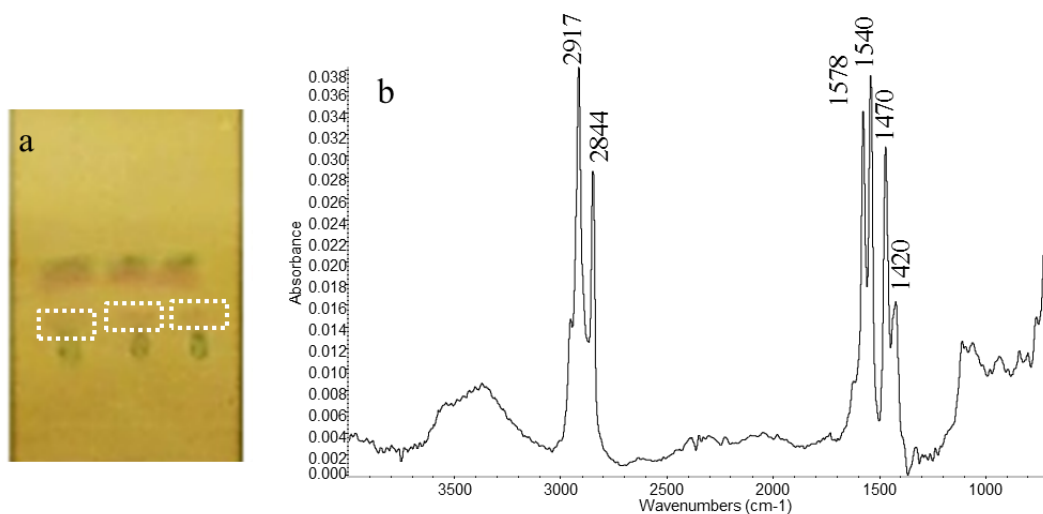
# DYE MIXTURE B



### MU-ATR SPECTRA

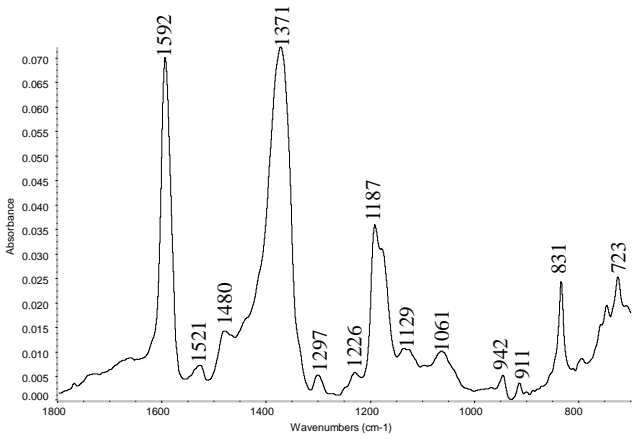
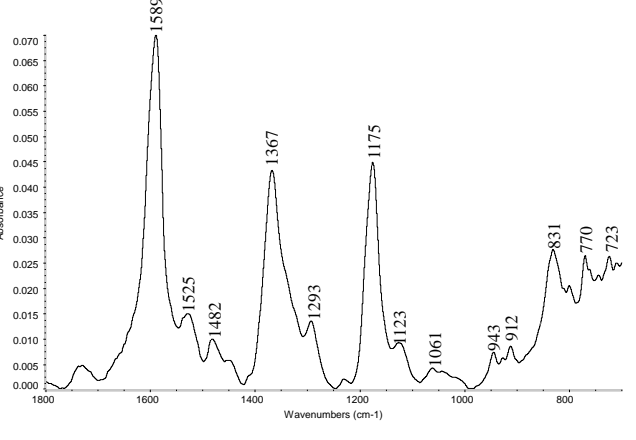
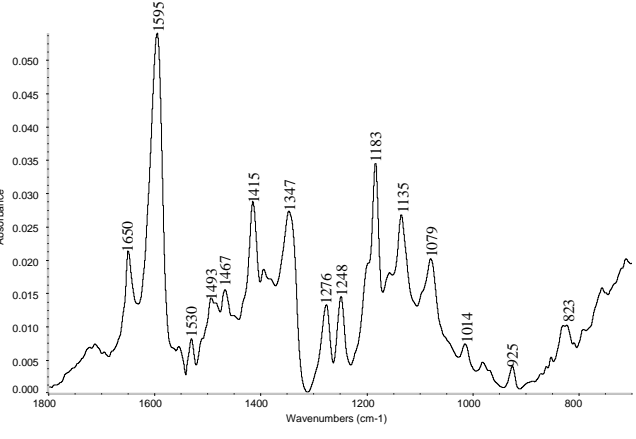


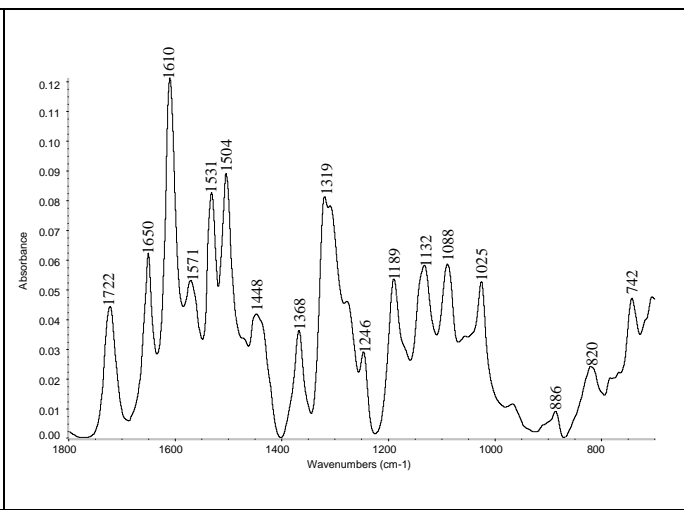
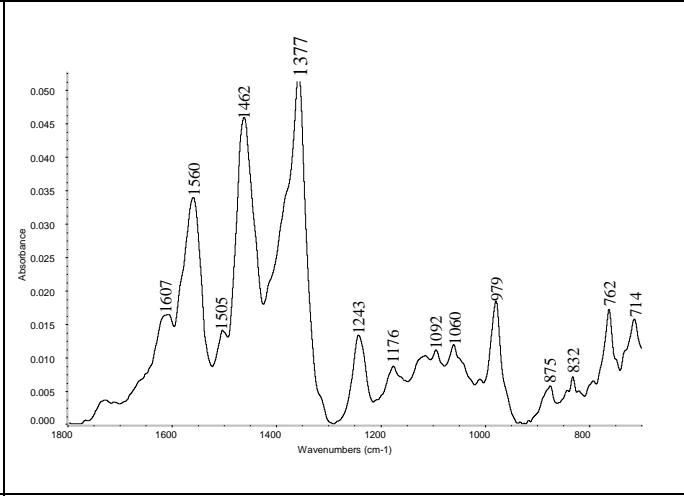
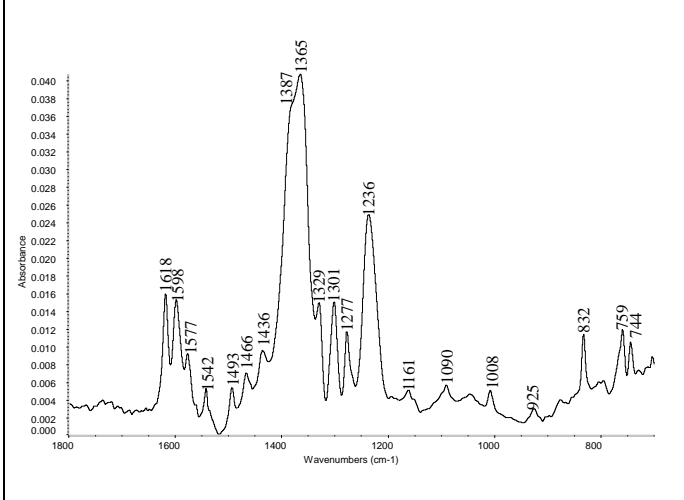
**SI Figure 4.** SERS and MU-ATR spectra of the dye mixtures A and B after the TLC separation.

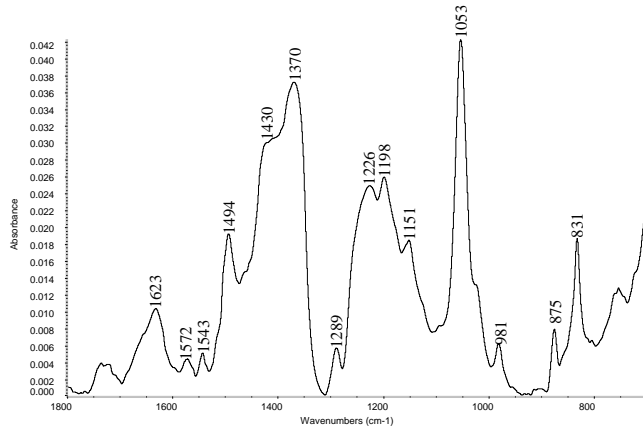


**SI Figure 5:** a) Dye mixture extracted from the dyed wool after TLC development on AgI@Au plate. White squares indicate areas where the carboxylates have been identified; b) MU-ATR spectrum

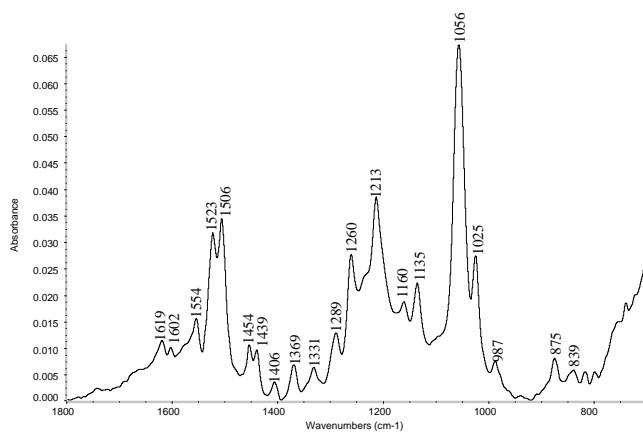
Dye Code	MU-ATR Spectrum on AgI@Au plate	Tentative bands assignments
BG1	<p>The spectrum for dye BG1 shows absorbance on the y-axis (0.000 to 0.080) and wavenumber on the x-axis (1800 to 800 cm-1). Key peaks are labeled at 1618, 1587, 1449, 1419, 1385, 1345, 1275, 1187, 1157, 1075, 1005, 937, 900, 830, and 750 cm-1.</p>	<p>1618: aromatic C=C stret.<sup>1</sup>; 1587: C=C str.; 1517: C=C ring str. <sup>1</sup>; 1449: CH<sub>3</sub> def<sup>1</sup>; 1419: CH<sub>2</sub> scissoring def, N-H in plane def; 1385: CH<sub>3</sub> def<sup>1</sup>, N-H in plane def. <sup>1</sup>; 1187: C-C str. <sup>1</sup>, CH<sub>2</sub> wagging<sup>1</sup>; 1157: HSO<sub>3</sub>- ion<sup>1</sup>; 1075: HSO<sub>3</sub>- ion S-O sym. Str., C-H in-plane bend.; NH<sub>2</sub> rock<sup>1</sup>; 1005: SO<sub>3</sub>Na sym str<sup>1</sup>, asym C-C-N ring bend.<sup>1</sup></p>

<p><b>BV3</b></p>	 <p>IR spectrum showing Absorbance vs Wavenumbers (cm<sup>-1</sup>). Key peaks are labeled: 1592, 1521, 1480, 1371, 1297, 1226, 1187, 1129, 1061, 942, 911, 831, 723.</p>	<p>1592: C=C ring str.<sup>1</sup>; 1521: C=C ring<sup>1</sup> str.; 1480: CH<sub>3</sub> def.; 1297: C-N str.; 1226: Asym C-N str.<sup>1</sup>; 1129: CH in-plane bend<sup>1</sup>; 723: Sym CArCArN str.</p>
<p><b>BV1</b></p>	 <p>IR spectrum showing Absorbance vs Wavenumbers (cm<sup>-1</sup>). Key peaks are labeled: 1589, 1525, 1482, 1367, 1293, 1175, 1123, 1061, 943, 912, 831, 770, 723.</p>	<p>1589: C=C str. ; aromatic C=C str<sup>1</sup>; 1525: C=C str ring<sup>1</sup>; 1482: CH<sub>3</sub> def<sup>1</sup>; 1293: C-N str<sup>1</sup>; 1122: CH in plane bend<sup>1</sup>; 912: Sym. C-N str.<sup>1</sup>; 723: CH<sub>3</sub> wagging; C-C out-of-plane bend<sup>1</sup>.</p>
<p><b>BV10</b></p>	 <p>IR spectrum showing Absorbance vs Wavenumbers (cm<sup>-1</sup>). Key peaks are labeled: 1650, 1595, 1530, 1493, 1467, 1415, 1347, 1276, 1248, 1183, 1135, 1079, 1014, 925, 823, 723.</p>	<p>1650: Xanth ring str<sup>2,3</sup>; 1595: Xanth ring str<sup>3</sup>; 1530: Xanth ring -NHC<sub>2</sub>H<sub>5</sub> str<sup>4</sup>; 1347: Xanth. ring C-C str.; 1276: Phen. group<sup>2</sup>, C-H bend<sup>3</sup>; 1248: Xanth ring -Phen.<sup>4</sup>; 1183: C-H bend<sup>3</sup>; 1135: Xanth ring -NHC<sub>2</sub>H<sub>5</sub><sup>2</sup>; 1079: Phen ring str<sup>3</sup>; 925: Xanth ring -NHC<sub>2</sub>H<sub>5</sub>-phen<sup>2</sup>; 823: Xanth ring -NHC<sub>2</sub>H<sub>5</sub>-phen<sup>2</sup>.</p>

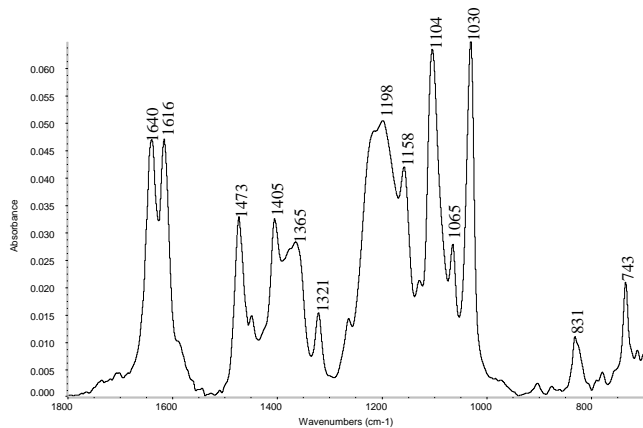
<p><b>BR1</b></p>		<p>1722: C=O str.<sup>4</sup>; 1650: Xanth ring str.<sup>4</sup>; 1610: Xanth ring str; 1570 phen. str.<sup>4</sup>; 1448: C=O str.<sup>4</sup>; 1368: COO<sup>-</sup> str.; 1319: Xanth. ring CC str.; 1189: Xanth ring str.<sup>4</sup>.</p>
<p><b>AR87</b></p>		<p>1607: Xanth ring str.<sup>6,7</sup>; 1560: Xanth ring str.<sup>6</sup>; 1462: C=O str.<sup>7</sup>; 1377: COO<sup>-</sup> str.; 1243: C-H in-plane bend<sup>6</sup>; 979: C-H out-of-plane bend<sup>6,7</sup>; 762: C-H out-of-plane bend<sup>6,7</sup>; 714: C-H out-of-plane bend<sup>6,7</sup>.</p>
<p><b>AY2<sup>8</sup></b></p>		<p>1618: aromatic C=C str, C-N bend; 1598: NO<sub>2</sub> rock., aromatic C=C str; 1577: NO<sub>2</sub> sym str.; 1496: aromatic C-C str.; 1387: aromatic C-C str., NO<sub>2</sub> sym str., 1329: NO<sub>2</sub> sym str, NO<sub>2</sub> sym bend., NO<sub>2</sub> rock., C-N str.; 1301: RC-H bend, aromatic C-C str.; 1277: RC-H bend, R1 trigonal def.; 1240: RC-H bend, C-O bend.; 759: R1 asym. torsion, C-H wag, R1 puckering, CN wagging; 744: C-N bend., aromatic C-C str., NO<sub>2</sub> sym bend., C-O bend.</p>

**AR18**<sup>9</sup>

1543: N-H bend., C=N str., C-C str., N-H bend.; 1494: N-H bend., C-O str., C=N str.; 1430: N=N str.; 1370: C-C str., C-N str.; 1289: C-N str, C-H in-plane bend.; 1198: Asym. str., SO<sub>3</sub><sup>-</sup>, C-S str.; 1151: C-S, SO<sub>3</sub>; 1053: Sym. Str. SO<sub>3</sub><sup>-</sup>, C-S str.; 831: C-H out-of-plane def.

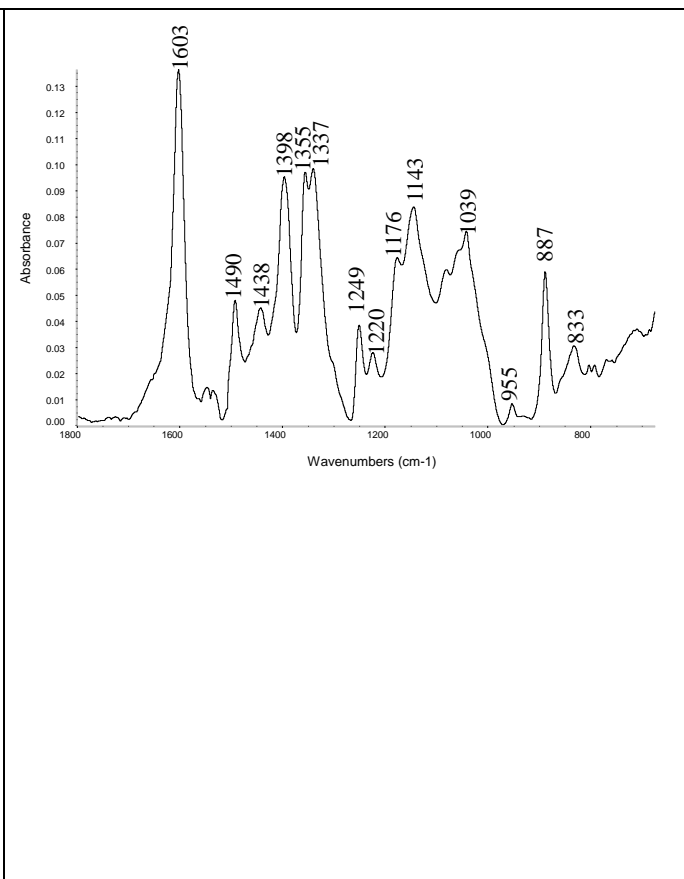
**AR88**

1619: N=N str.<sup>10</sup>; 1523: aromatic C=C str. <sup>10</sup>; 1506: aromatic C=C str. <sup>10</sup>; 1368: N=N str. <sup>11</sup>; 1160: C-O str.; 1213: C-O str.; 1056: S=O str. <sup>11</sup>; 839: C-H out-of plane bend. <sup>10</sup>

**AB74**

1640: aromatic C=C str. <sup>12</sup>; 1615: C=C str.; <sup>12</sup>, <sup>13</sup>; 1104: asym. benzenesulfonic acids str. <sup>13</sup>; 1030 SO<sub>3</sub> str; <sup>12</sup>.



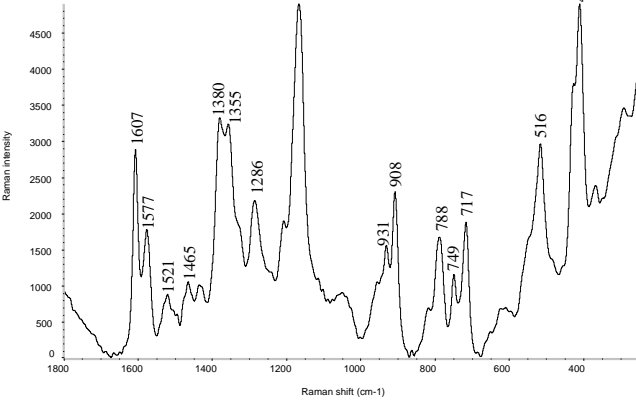
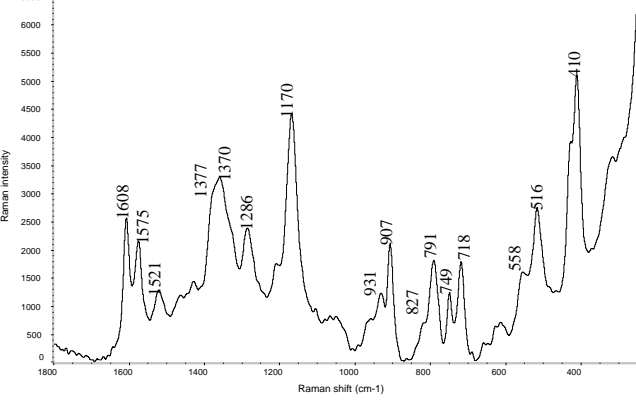
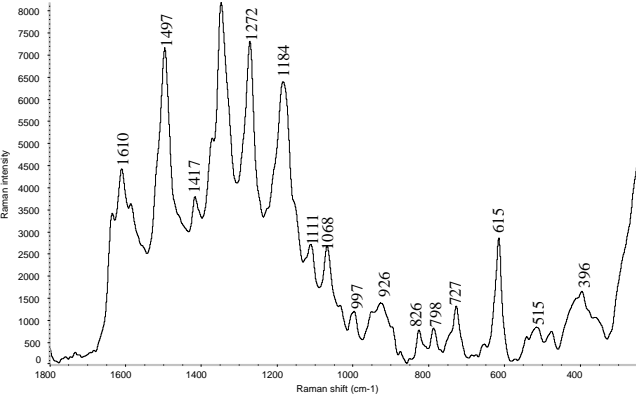
<b>BB9</b>		<p>1603: Aromatic C=C str.<sup>14</sup>; antisym. C-N str.<sup>15</sup>; C=C str.<sup>13</sup>; C-H in-plane bend.<sup>15</sup>; 1490: C=N str.; C=C str.; C-H out of plane bend.<sup>15</sup>; 1438: Asym. C-H bend.<sup>16</sup>; antisym. C-N str.<sup>15</sup>; C-H in-plane bend.<sup>15</sup>; out-of-plane C-H bend.<sup>15</sup>; 1398: sym. C-H bend.; sym. C-H bend.<sup>16</sup>; antisym. C-N str.<sup>16</sup>; C-H in-plane bend.<sup>16</sup>; C-H out-of-plane bend.<sup>16</sup>; 1355: sym. Ar-N str.<sup>14</sup>; C-H in-plane bend.<sup>15</sup>; C-H out-of-plane bend.<sup>15</sup>; 1249: C-H in-plane bend.<sup>16</sup>; 1220: antisym. C-N str.<sup>15</sup>; C-H in plane bend.<sup>16</sup>; C-H out-of-plane bend.<sup>15</sup>; 1176: C-H out-of-plane bend.<sup>16</sup>; C-H in-plane bend.<sup>15</sup>; 1143: C-H in plane bend.<sup>15</sup>; 1039: antisym. C-S str.<sup>15</sup>; C-H in plane bend.<sup>15</sup>; 887: C-H bend.<sup>15</sup>; C-H out of plane bend.<sup>15</sup></p>
------------	--	---

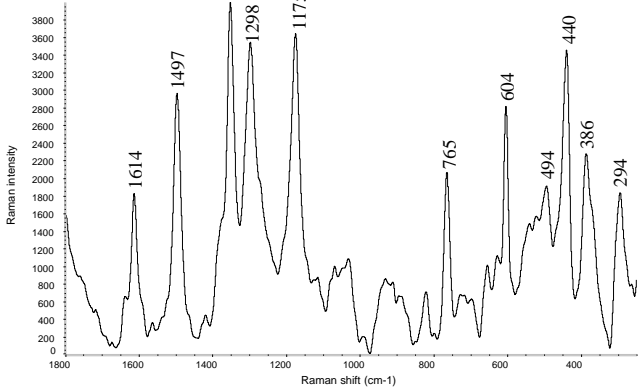
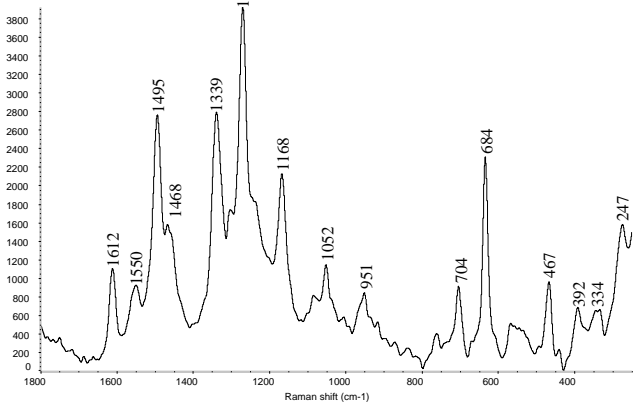
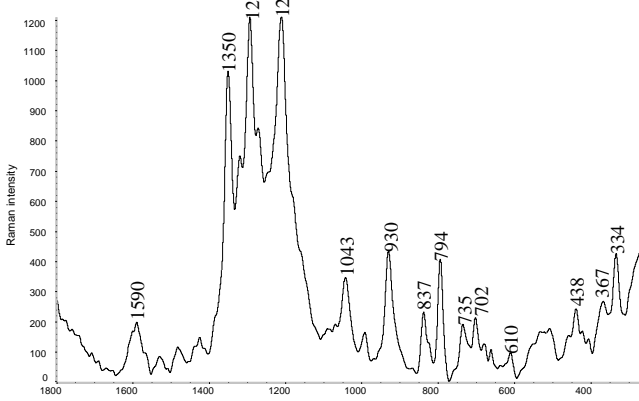
**SI Table 1.** MU-ATR spectra of the investigated synthetic dyes on AgI@Au TLC plates

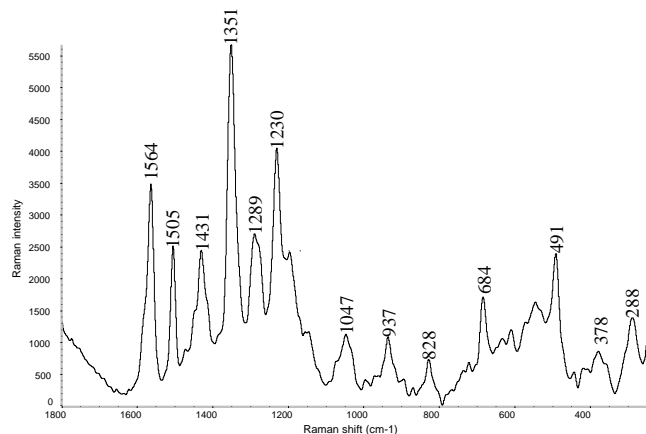
1. Doherty, B., Vagnini, M., Dufourmantelle, K., Sgamellotti, A., Brunetti, B., & Miliani, C. (2014). A vibrational spectroscopic and principal component analysis of triarylmethane dyes by comparative laboratory and portable instrumentation. *Spectrochimica Acta Part A: Molecular and Biomolecular Spectroscopy*, 121, 292-305.
2. Sharma A., Kumar A., Vibrational (2013)study of Rhodamine 610 and effect of methanol on its vibrational spectra; *Greener Journal of Physical Sciences* 3(6), 200-203.
3. Sarkar, J., Chowdhury, J., Pal, P., & Talapatra, G. B. (2006). Ab initio, DFT vibrational calculations and SERRS study of Rhodamine 123 adsorbed on colloidal silver particles. *Vibrational spectroscopy*, 41(1), 90-96.
4. Watanabe, H., Hayazawa, N., Inouye, Y., & Kawata, S. (2005). DFT vibrational calculations of rhodamine 6G adsorbed on silver: analysis of tip-enhanced Raman spectroscopy. *The Journal of Physical Chemistry B*, 109(11), 5012-5020.
5. Narayanan, V. A., Stokes, D. L., & Vo-Dinh, T. (1994). Vibrational spectral analysis of Eosin Y and Erythrosin B—intensity studies for quantitative detection of the dyes. *Journal of Raman spectroscopy*, 25(6), 415-422.
6. Hazebroucq, S., Labat, F., Lincot, D., & Adamo, C. (2008). Theoretical insights on the electronic properties of eosin Y, an organic dye for photovoltaic applications. *The Journal of Physical Chemistry A*, 112(31), 7264-7270.
7. Markuszewski, R., & Diehl, H. (1980). The infrared spectra and structures of the three solid forms of fluorescein and related compounds. *Talanta*, 27(11), 937-946.
8. Snehalatha, M., Ravikumar, C., Joe, I. H., & Jayakumar, V. S. (2009). Vibrational spectra and scaled quantum chemical studies of the structure of Martius yellow sodium salt monohydrate. *Journal of Raman Spectroscopy*, 40(9), 1121-1126.

9. Almeida, M. R., Stephani, R., Dos Santos, H. F., & Oliveira, L. F. C. D. (2009). Spectroscopic and theoretical study of the “azo”-dye E124 in condensate phase: evidence of a dominant hydrazo form. *The Journal of Physical Chemistry A*, 114(1), 526-534.
10. Dikmen, S., Gunay, A., Ersoy, B., & Erol, I. (2015). DETERMINATION OF THE EQUILIBRIUM, KINETIC AND THERMODYNAMIC PARAMETERS OF ACID RED 88 ADSORPTION ONTO MONTMORILLONITIC CLAY. *Environmental Engineering and Management Journal*, 14(5), 1097-1110.
11. Anil Kumar, M., Vinoth Kumar, V., Ponnusamy, R., Paul Daniel, F., Seenuvasan, M., Anuradha, D., & Sivanesan, S. (2015). Concomitant mineralization and detoxification of acid red 88 by an indigenous acclimated mixed culture. *Environmental Progress & Sustainable Energy*, 34(5), 1455-1466.
12. Vautier, M., Guillard, C., & Herrmann, J. M. (2001). Photocatalytic degradation of dyes in water: case study of indigo and of indigo carmine. *Journal of Catalysis*, 201(1), 46-59.
13. Galindo, C., Jacques, P., & Kalt, A. (2001). Photochemical and photocatalytic degradation of an indigoid dye: a case study of acid blue 74 (AB74). *Journal of Photochemistry and Photobiology A: Chemistry*, 141(1), 47-56.
14. Sáez, E. I., & Corn, R. M. (1993). In situ polarization modulation—Fourier transform infrared spectroelectrochemistry of phenazine and phenothiazine dye films at polycrystalline gold electrodes. *Electrochimica acta*, 38(12), 1619-1625.
15. Aoki, P. H., Volpati, D., Caetano, W., & Constantino, C. J. (2010). Study of the interaction between cardiolipin bilayers and methylene blue in polymer-based Layer-by-Layer and Langmuir films applied as membrane mimetic systems. *Vibrational Spectroscopy*, 54(2), 93-102.
16. Ovchinnikov, O. V., Chernykh, S. V., Smirnov, M. S., Alpatova, D. V., Vorob'Eva, R. P., Latyshev, A. N., ... & Lukin, A. N. (2007). Analysis of interaction between the organic dye methylene blue and the surface of AgCl (I) microcrystals. *Journal of Applied Spectroscopy*, 74(6), 809-816.

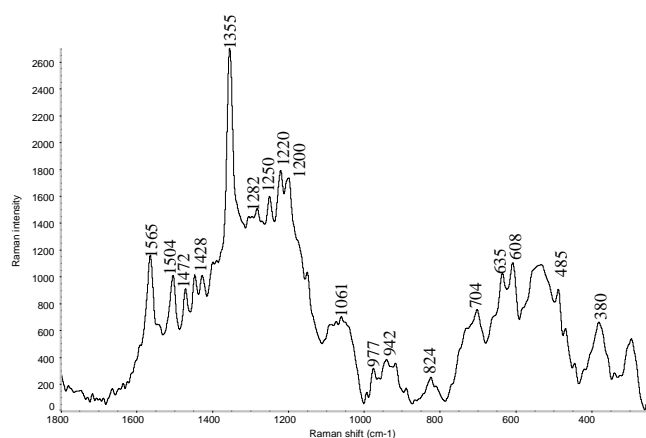
Dye Code	SERS-Raman Spectrum on AgI@Au plate	Tentative bands assignments
BG1		1607: aromatic C-C str. <sup>1</sup> ; 1528: C-N str.; sym. CH <sub>3</sub> bend. <sup>1</sup> ; 1481: asym. C-H bend. <sup>1</sup> ; 1374: C-C str. <sup>1</sup> ; 1357: asym. C-C str.; C-C bend.; C-H bend. <sup>1</sup> ; 1272: asym. C-C str.; C-C bend. <sup>2</sup> ; C-H bend. <sup>1</sup> ; 1210: sym. C-C str.; C-C bend.; C-H bend. <sup>2</sup> ; 1176: C-H bend. <sup>1</sup> ; 1150: sym. C-C str.; C-C bend.; C-H bend. <sup>1</sup> ; 995: C-C bend. <sup>2</sup> ; 904: C-C str. <sup>1</sup> ; 788: C-C str.; C-N str. <sup>1</sup> ; 736: C-N str. <sup>1</sup> ; 430: C-N bend.; 414: CNC bend.; C-C bend., SO <sub>3</sub>

		bend. <sup>2</sup>
<b>BV3<sup>1</sup></b>	 <p>Raman spectrum for BV3. The x-axis is Raman shift (cm<sup>-1</sup>) from 1800 to 400, and the y-axis is Raman intensity from 0 to 4500. Key peaks are labeled at 1607, 1577, 1521, 1465, 1380, 1355, 1286, 1167, 931, 908, 788, 749, 717, 516, and 410 cm<sup>-1</sup>.</p>	1607: aromatic C-C str.; 1577: aromatic C-C str.; 1380: C-C str.; 1355: asym. C-C str., C-C-C ring bend.; C-H bend.; 1171: sym. C-C str.; C-C-C bend.; C-H bend.; 908: C-C ring str.; 717: C-N str.; 410: C-N-C bend.; C-C-C bend.
<b>BV1<sup>1</sup></b>	 <p>Raman spectrum for BV1. The x-axis is Raman shift (cm<sup>-1</sup>) from 1800 to 400, and the y-axis is Raman intensity from 0 to 6500. Key peaks are labeled at 1608, 1575, 1521, 1377, 1370, 1286, 1170, 931, 907, 827, 791, 749, 718, 558, 516, and 410 cm<sup>-1</sup>.</p>	1584: aromatic C-C str.; 1170: sym. C-C-C str.; C-C-C bend.; C-H bend; 907: C-C ring str.; 797: sym. C-C-C str.; C-N str.;
<b>BV10</b>	 <p>Raman spectrum for BV10. The x-axis is Raman shift (cm<sup>-1</sup>) from 1800 to 400, and the y-axis is Raman intensity from 0 to 8000. Key peaks are labeled at 1610, 1497, 1417, 1348, 1272, 1184, 1111, 1008, 997, 926, 826, 798, 727, 615, 515, and 396 cm<sup>-1</sup>.</p>	1610: Xhant. ring str. <sup>3</sup> ; 1497: Xhant. ring str. <sup>3</sup> ; 1348: Xhant. ring str. <sup>3</sup> ; 1272: C-H bend. <sup>3</sup> ; 1180: C-H bend.; 924: Xhant. ring + phenyl str.; 727: C-H out-of-plane bend. of phenyl ring.; 615: Xanth. ring in.plane def. <sup>4</sup>

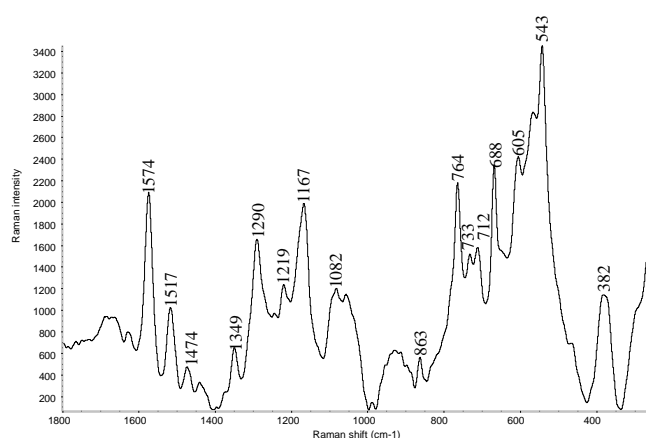
<p><b>BR1<sup>4</sup></b></p>		<p>1497: Xanth. ring str.; C-N str.; C-H bend.; N-H bend.; 1353: Xanth. Ring str.; C-H in-plane bend.; 1298: Xanth. Ring def.; N-H bend.; CH<sub>2</sub> wagging.; 1175: Xanth. ring in-plane def.; C-H bend.; N-H bend.; 765: Xanth. ring in-plane def.; 604: Xanth. ring in-plane def.</p>
<p><b>AR87<sup>5</sup></b></p>		<p>1612: Xanth. C-C ring str.; 1495: Xanth. C-C ring str.; 1339 Xanth. C-C ring str.; 1270: C-C str.; 1052: C-C str.; sym C-O str.; 1270: Xanth. and Bz C-C ring str. 1052: Bz ring str.; sym. CO<sub>2</sub> str.; 704: Xanth. out-of-plane ring def.</p>
<p><b>AY2<sup>6</sup></b></p>		<p>1211: Naphthalene C-H bend. ; 1143: C-H out-of-plane bend. 1350: C-C str.; 930: NO<sub>2</sub> def.; 702: NO<sub>2</sub> def.</p>

**AR18<sup>7</sup>**

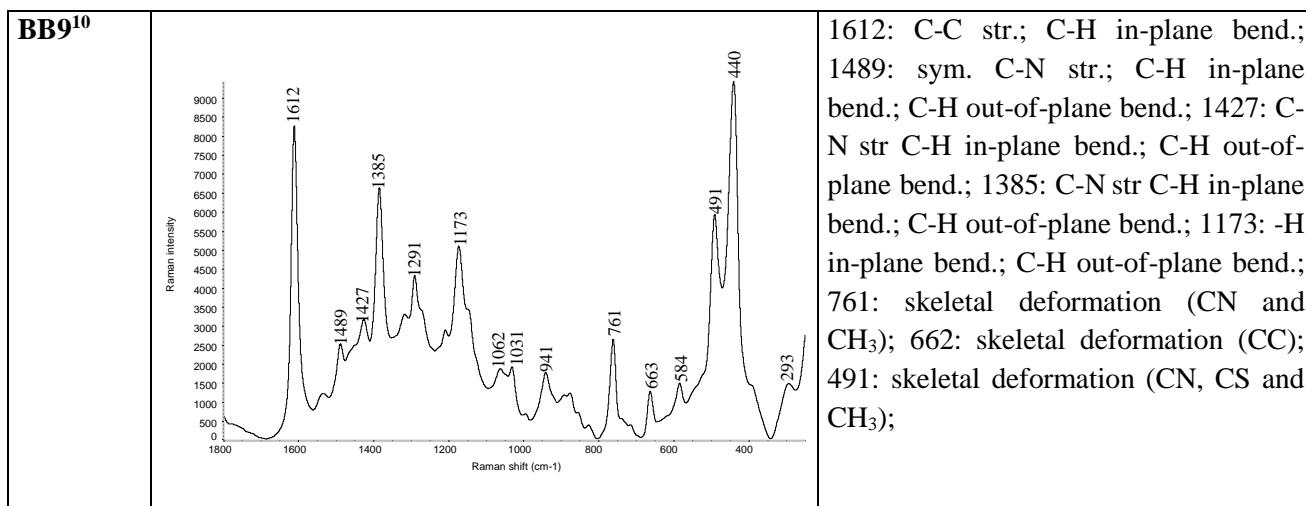
1564: aromatic C=C str.; N-H bend.;  
 1503: C=O str., C=N str.; N-H bend.;  
 1431: C-H str.; 1351: C-C str.; 1289: N-N str.; C-C str.; 1230: C-C str.; N-N str.;  
 491: out-of-plane ring def.

**AR88<sup>8</sup>**

1565: aromatic C=C str.; 1355: N=N str.;  
 1200: sym. C-N str.

**AB74<sup>9</sup>**

1584: Asym. C=C str.; C=O str.; C=N str.;  
 1474: C-C str.; C-H bend.; C=N str.;  
 1290: sym. SO<sub>3</sub> str.; C-C bend.;  
 1082: O-Na bend.; C-H bend.; C-C bend.;  
 863: N-H bend.; C-N str.; 543: (C=C-CO-C) bend.



**SI Table 2.** Raman spectra of the investigated synthetic dyes on AgI@Au TLC plate

1. Doherty, B., Vagnini, M., Dufourmantelle, K., Sgamellotti, A., Brunetti, B., & Miliani, C. (2014). A vibrational spectroscopic and principal component analysis of triarylmethane dyes by comparative laboratory and portable instrumentation. *Spectrochimica Acta Part A: Molecular and Biomolecular Spectroscopy*, *121*, 292-305.
2. Wu, M. C., Lin, M. P., Chen, S. W., Lee, P. H., Li, J. H., & Su, W. F. (2014). Surface-enhanced Raman scattering substrate based on a Ag coated monolayer array of SiO<sub>2</sub> spheres for organic dye detection. *RSC Advances*, *4*(20), 10043-10050.
3. Sarkar, J., Chowdhury, J., Pal, P., & Talapatra, G. B. (2006). Ab initio, DFT vibrational calculations and SERRS study of Rhodamine 123 adsorbed on colloidal silver particles. *Vibrational spectroscopy*, *41*(1), 90-96.
4. Jensen, L., & Schatz, G. C. (2006). Resonance Raman scattering of rhodamine 6G as calculated using time-dependent density functional theory. *The Journal of Physical Chemistry A*, *110*(18), 5973-5977.
5. Greeneltch, N. G., Davis, A. S., Valley, N. A., Casadio, F., Schatz, G. C., Van Duyne, R. P., & Shah, N. C. (2012). Near-infrared surface-enhanced Raman spectroscopy (NIR-SERS) for the identification of Eosin Y: theoretical calculations and evaluation of two different nanoplasmonic substrates. *The Journal of Physical Chemistry A*, *116*(48), 11863-11869.
6. Snehalatha, M., Ravikumar, C., Joe, I. H., & Jayakumar, V. S. (2009). Vibrational spectra and scaled quantum chemical studies of the structure of Martius yellow sodium salt monohydrate. *Journal of Raman Spectroscopy*, *40*(9), 1121-1126.
7. Almeida M.R., (2010) Spectroscopic and Theoretical Study of the “Azo”-Dye E124 in Condensate Phase: Evidence of a Dominant Hydrazo Form, *The Journal of Physical Chemistry A* *114*, 526-534.
8. Schulte, F., Brzezinka, K. W., Lutzenberger, K., Stege, H., & Panne, U. (2008). Raman spectroscopy of synthetic organic pigments used in 20th century works of art. *Journal of Raman spectroscopy*, *39*(10), 1455-1463.
9. Peica, N., & Kiefer, W. (2008). Characterization of indigo carmine with surface-enhanced resonance Raman spectroscopy (SERRS) using silver colloids and island films, and theoretical calculations. *Journal of Raman Spectroscopy*, *39*(1), 47-60.
10. Aoki, P. H., Volpati, D., Caetano, W., & Constantino, C. J. (2010). Study of the interaction between cardiolipin bilayers and methylene blue in polymer-based Layer-by-Layer and Langmuir films applied as membrane mimetic systems. *Vibrational Spectroscopy*, *54*(2), 93-102.